Commun. Comput. Phys.
doi: 10.4208/cicp.300810.140411s

Vol. **11**, No. 4, pp. 1261-1278
April 2012

An Adaptive Time-Stepping Strategy for the Cahn-Hilliard Equation

Zhengru Zhang[1] and Zhonghua Qiao[2,*]

[1] *Laboratory of Mathematics and Complex Systems, Ministry of Education; School of Mathematical Sciences, Beijing Normal University, Beijing 100875, China.*
[2] *Institute for Computational Mathematics & Department of Mathematics, Hong Kong Baptist University, Kowloon Tong, Hong Kong.*

Received 30 August 2010; Accepted (in revised version) 14 April 2011

Available online 29 November 2011

Abstract. This paper studies the numerical simulations for the Cahn-Hilliard equation which describes a phase separation phenomenon. The numerical simulation of the Cahn-Hilliard model needs very long time to reach the steady state, and therefore large time-stepping methods become useful. The main objective of this work is to construct the unconditionally energy stable finite difference scheme so that the large time steps can be used in the numerical simulations. The equation is discretized by the central difference scheme in space and fully implicit second-order scheme in time. The proposed scheme is proved to be unconditionally energy stable and mass-conservative. An error estimate for the numerical solution is also obtained with second order in both space and time. By using this energy stable scheme, an adaptive time-stepping strategy is proposed, which selects time steps adaptively based on the variation of the free energy against time. The numerical experiments are presented to demonstrate the effectiveness of the adaptive time-stepping approach.

AMS subject classifications: 35L64, 65M93, 65M30

Key words: Adaptive time-stepping, unconditionally energy stable, Cahn-Hilliard equation, mass conservation.

1 Introduction

The Cahn-Hilliard equation arises as a phenomenological continuum model for the two mixture components and was originally introduced in [1]:

*Corresponding author. *Email addresses:* zrzhang@bnu.edu.cn (Z. R. Zhang), zqiao@hkbu.edu.hk (Z. H. Qiao)

$$\frac{\partial u}{\partial t}+\Delta(u-u^3+\kappa\Delta u)=0, \qquad (\boldsymbol{x},t)\in\Omega\times\mathrm{R}^+, \tag{1.1a}$$

$$u(\boldsymbol{x},0)=u_0(\boldsymbol{x}), \qquad \boldsymbol{x}\in\Omega, \tag{1.1b}$$

$$u(\cdot,t) \text{ is subject to periodic boundary condition,} \tag{1.1c}$$

where the domain $\Omega=(0,L_1)\times(0,L_2)$ is an open set in R^2, κ is a positive constant and $u_0(\boldsymbol{x})$ is a given function.

There have been an enormous amount of research work, and still growing, on the mathematical and numerical analysis of the Cahn-Hilliard equation. In [2, 14] the steady state solutions of the Cahn-Hilliard equation were studied. Elliott and Zheng proved the existence and uniqueness of the solution for the Cahn-Hilliard equation in [6]. It is difficult to find the analytical solutions, so many efforts have been made on the numerical simulations for the Cahn-Hilliard equation recently. Finite element methods have been first studied on solving the Cahn-Hilliard equation by Elliott et al. in [7–9]. In [5], Du and Nicolaides proposed a fully finite element method and proved the convergence without assumptions beyond those necessary for existence and uniqueness of the differential equation. In [17], a linearized finite difference scheme was derived using the method of reduction of order. Solvability and convergence were studied, but the mass conservation is not preserved and only conditional stability was obtained. In [4], a conservative nonlinear finite difference scheme was proposed, which is unconditionally stable in L^∞-norm and conserves the total mass. However, the energy-based stability was not discussed. In [10], a conservative difference method was proposed for solving the one-dimensional Cahn-Hilliard equation and it was proved to be unconditionally stable in the sense of energy decay. Most recently, an unconditionally stable finite difference scheme was developed to solve the Cahn-Hilliard-Hele-Shaw system of equations in [19].

Since the simulation of Cahn-Hilliard model needs very long time to reach the steady state, the large time-stepping method is needed. In [11], a large time-stepping method was proposed for simulating the Cahn-Hilliard equation. The time step can be increased by adding a linear term to the classical semi-implicit finite difference scheme. However, the adding term is dependent on the unknown numerical solution. In [20], the same large time-stepping method was applied to the epitaxial growth models. In [21], a nonconforming finite element method coupled with the convexity-splitting scheme for the discretization in temporal variable was proposed to solve the Cahn-Hilliard equation. An artificial extra term was also introduced to adjust the dissipation of the energy, which was dependent on the unknown numerical solution.

In this paper, we present a finite difference scheme for solving the two-dimensional Cahn-Hilliard equation, which discretizes the equation by the central difference scheme in space and fully implicit second order scheme in time. The stability and error estimate will be analyzed. It will be proved that this finite difference scheme is unconditionally energy stable and mass-conservative, which guarantees that the large time steps can be used in the numerical simulations of the Cahn-Hilliard equation. However, constant

large time steps may cause accuracy loss especially during the stage of the large solution variation. To overcome this disadvantage, we propose an adaptive time-stepping strategy with which the time step varies according to the evolution of the energy. As we know, the energy is an important quantity in the Cahn-Hilliard equation. The adaptive time steps are selected based on the variation of the energy against time. When the energy varies rapidly, the small time step is used. If the energy varies slowly and smoothly, the large time step is used. The free energy of the Cahn-Hilliard model is defined as

$$E(u)=\frac{\kappa}{2}\|\nabla u\|^2+\frac{1}{4}\|u^2-1\|^2.$$

In [15], this time-stepping strategy has been successfully used for solving the epitaxial growth models.

Adaptive time-stepping techniques have been well studied for ODEs and PDEs in various of forms. In [16], several time step control methods for the local time adaptivity based on the linear feedback theory were reviewed. These time step adaptivity methods are aimed to improve the numerical accuracy. Therefore it has limited advantage to increase the computational efficiency. In [13], two adaptive time methods are compared with constant time steps for coupled flow and deformation models. In their work, the pore pressure method is an inexpensive adaptive method whose behavior closely follows the physics of the problem, while the local error method is more time-consuming at each time step because feedback steps may be involved. In [18], a locally varying time step method was proposed for solving hyperbolic conservation laws and convection-diffusion equations. At the same time level, a larger time step is used in the region with the smooth solution, while a smaller time step is adopted in the region where the solution is singular or nearly singular. In [3], an adaptive time-stepping strategy based on the power law was presented to control the accuracy of the unconditionally stable schemes for the Cahn-Hilliard equation.

The outline of this paper is as follows. In Section 2, we give the nonlinear difference scheme and show that the proposed scheme preserves the total mass and energy identities unconditionally in the discrete sense. The L^∞-norm stability is obtained and the error estimate with the order $\mathcal{O}((\Delta x)^2+(\Delta y)^2+(\Delta t)^2)$ is analyzed. In Section 3, an adaptive time-stepping technique is proposed to improve the computational efficiency. The time step indicator is dependent on the time derivative of the energy functional. In Section 4, numerical experiments are carried out to support the effectiveness of the proposed scheme. The paper ends with some conclusions in Section 5.

2 Unconditionally energy stable scheme

Lemma 2.1. *Let $u(\boldsymbol{x},t)$ be the solution of the Cahn-Hilliard equation* (1.1a)-(1.1c)*, then the mass conservation holds* [1, 12],

$$\frac{d}{dt}\int_\Omega u(\boldsymbol{x},t)d\boldsymbol{x}=0,\quad 0\le t\le T. \tag{2.1}$$

We briefly sketch the proof of (2.1). Integrating both sides of (1.1a) over the domain Ω, by Green's theorem and periodic boundary conditions, the result (2.1) is obtained.

Lemma 2.2. *Let $u(\boldsymbol{x},t)$ be the solution of the Cahn-Hilliard equation* (1.1a)-(1.1c)*, then the following energy identity holds* [1, 12]*,*

$$\frac{dE(u)}{dt}+\|\nabla\mu\|^2=0, \tag{2.2}$$

where $\mu=u-u^3+\kappa\Delta u$.

A brief proof is as below. It follows from (1.1a) that

$$\left(\frac{\partial u}{\partial t},\varphi\right)=(-\Delta\mu,\varphi),$$

where $(\cdot,\cdot)$ denotes the standard inner product in the L^2-space. It can be verified directly that setting $\varphi=\mu$ yields (2.2). Here Green's theorem and periodic boundary conditions are used again.

Let N_x, N_y be positive integers. The domain Ω is uniformly partitioned with $\Delta x = L_1/N_x$ and $\Delta y = L_2/N_y$ and

$$\bar{\Omega}_h=\left\{(x_j,y_k)|x_j=j\Delta x,\ y_k=k\Delta y,\ 0\le j\le N_x,\ 0\le k\le N_y\right\}.$$

The time step is denoted by Δt.

For a given two-dimensional grid function $\{f_{j,k}\}$, we define the following discrete difference operator

$$\nabla_h f_{j+\frac{1}{2},k+\frac{1}{2}}=\begin{pmatrix}\dfrac{f_{j+1,k}-f_{j,k}}{\Delta x}\\ \dfrac{f_{j,k+1}-f_{j,k}}{\Delta y}\end{pmatrix},\quad \Delta_h f_{j,k}=\frac{f_{j+1,k}-2f_{j,k}+f_{j-1,k}}{(\Delta x)^2}+\frac{f_{j,k+1}-2f_{j,k}+f_{j,k-1}}{(\Delta y)^2}.$$

The discrete L^2 inner product and the discrete L^2-norm are defined as

$$(f,g)_h=\sum_{j=1}^{N_x}\sum_{k=1}^{N_y}f_{j,k}g_{j,k}\Delta x\Delta y,\qquad \|f\|_h^2=(f,f)_h.$$

The discrete H^1-norm is defined as

$$\|f\|_{H^1,h}=\left[\sum_{j=1}^{N_x}\sum_{k=1}^{N_y}\left(|f_{j,k}|^2+\left|\nabla_h f_{j-\frac{1}{2},k-\frac{1}{2}}\right|^2\right)\Delta x\Delta y\right]^{\frac{1}{2}}.$$

Our finite difference scheme is

$$\frac{U_{j,k}^{n+1}-U_{j,k}^n}{\Delta t}+\Delta_h\mu_{j,k}^{n+\frac{1}{2}}=0,\quad 1\le j\le N_x,\ \ 1\le k\le N_y, \tag{2.3}$$

where

$$\mu_{j,k}^{n+\frac{1}{2}}=\frac{U_{j,k}^{n+1}+U_{j,k}^{n}}{2}-\frac{U_{j,k}^{n+1}+U_{j,k}^{n}}{2}\frac{(U_{j,k}^{n+1})^2+(U_{j,k}^{n})^2}{2}+\kappa\Delta_h\frac{U_{j,k}^{n+1}+U_{j,k}^{n}}{2}.$$

At the boundary grid points, periodic conditions are applied.

2.1 Mass conservation and energy decay

The finite difference scheme (2.3) preserves mass conservation and energy identities in the discrete sense, which is corresponding to the continuum cases in Lemmas 2.1 and 2.2.

Theorem 2.1. *For the solution of* (2.3)*, the discrete form of the mass conservation* (2.1) *holds, that is, for any* $0\leq n\leq N$*,*

$$\sum_{j=1}^{N_x}\sum_{k=1}^{N_y}\Delta x\Delta y U_{j,k}^{n+1}=\sum_{j=1}^{N_x}\sum_{k=1}^{N_y}\Delta x\Delta y U_{j,k}^{n}. \tag{2.4}$$

Proof. Multiplying $\Delta x\Delta y$ to both sides of (2.3) and summing for $j=1,\cdots,N_x$ and $k=1,\cdots,N_y$ and applying periodic boundary conditions, we get

$$\begin{aligned}
&\sum_{j=1}^{N_x}\sum_{k=1}^{N_y}U_{j,k}^{n+1}\Delta x\Delta y-\sum_{j=1}^{N_x}\sum_{k=1}^{N_y}U_{j,k}^{n}\Delta x\Delta y\\
=&-\Delta t\Delta x\Delta y\sum_{j=1}^{N_x}\sum_{k=1}^{N_y}\Delta_h\mu_{j,k}^{n+\frac{1}{2}}\\
=&-\Delta t\Delta x\Delta y\left(\sum_{j=1}^{N_x}\sum_{k=1}^{N_y}\frac{(\mu_{j,k+1}^{n+\frac{1}{2}}-\mu_{j,k}^{n+\frac{1}{2}})-(\mu_{j,k}^{n+\frac{1}{2}}-\mu_{j,k-1}^{n+\frac{1}{2}})}{(\Delta y)^2}\right.\\
&\left.+\sum_{j=1}^{N_x}\sum_{k=1}^{N_y}\frac{(\mu_{j+1,k}^{n+\frac{1}{2}}-\mu_{j,k}^{n+\frac{1}{2}})-(\mu_{j,k}^{n+\frac{1}{2}}-\mu_{j-1,k}^{n+\frac{1}{2}})}{(\Delta x)^2}\right)\\
=&0.
\end{aligned}$$

This completes the proof of (2.4). □

Theorem 2.2. *For any time step* $\Delta t>0$*, the discrete form of the energy identity* (2.2) *holds:*

$$\frac{E_h(U^{n+1})-E_h(U^n)}{\Delta t}+\|\nabla_h\mu^{n+\frac{1}{2}}\|_h^2=0, \tag{2.5}$$

where E_h *is the discrete energy functional defined as*

$$E_h(U)=\frac{\kappa}{2}\|\nabla_h U\|_h^2+\frac{1}{4}\|U^2-1\|_h^2.$$

Proof. Multiplying $\Delta t\mu_{j,k}^{n+\frac{1}{2}}$ to (2.3) and summing for $j=1,\cdots,N_x$ and $k=1,\cdots,N_y$ gives

$$\begin{aligned}
&(U^{n+1}-U^n,\mu^{n+\frac{1}{2}})_h=-\Delta t(\Delta_h\mu^{n+\frac{1}{2}},\mu^{n+\frac{1}{2}})_h=\Delta t\|\nabla_h\mu^{n+\frac{1}{2}}\|_h^2\\
&=\Big(U^{n+1}-U^n,\frac{U^{n+1}+U^n}{2}-\frac{U^{n+1}+U^n}{2}\frac{(U^{n+1})^2+(U^n)^2}{2}\Big)_h+\Big(U^{n+1}-U^n,\kappa\Delta_h\frac{U^{n+1}+U^n}{2}\Big)_h\\
&=\frac{1}{2}\|U^{n+1}\|_h^2-\frac{1}{2}\|U^n\|_h^2-\frac{1}{4}(\|U^{n+1}\|_{L^4,h}^4-\|U^n\|_{L^4,h}^4)-\Big(\frac{\kappa}{2}\|\nabla_hU^{n+1}\|_h^2-\frac{\kappa}{2}\|\nabla_hU^n\|_h^2\Big)\\
&=E_h(U^n)-E_h(U^{n+1}).
\end{aligned}\tag{2.6}$$

Therefore, it holds that

$$E_h(U^{n+1})-E_h(U^n)=-\Delta t\|\nabla_h\mu^{n+\frac{1}{2}}\|_h^2\le 0\tag{2.7}$$

for any time step $\Delta t>0$. □

Remark 2.1. Theorem 2.2 implies $E_h(U^{n+1})\le E_h(U^n)$ for any time steps. So the finite difference scheme (2.3) is unconditionally energy stable.

2.2 Stability analysis

The main purpose of this section is to show that if our proposed scheme has a solution, it is bounded in the maximum norm. The proof is based on the energy estimate (2.7) and discrete Sobolev Lemma.

Theorem 2.3. *The numerical solution of* (2.3) *is bounded in L^∞-norm by the initial data in the following form*

$$\|U^n\|_\infty\le\frac{C_1}{\sqrt{C_0}}\sqrt{E_h(U^0)+2L_1L_2},\tag{2.8}$$

where C_0 and C_1 are some constants.

Proof. Starting from the fact of discrete energy decay, we get

$$\begin{aligned}
E_h(U^0)&\ge E_h(U^n)\\
&=\sum_{j=1}^{N_x}\sum_{k=1}^{N_y}\Big(\frac{1}{4}(U_{j,k}^n)^4-\frac{1}{2}(U_{j,k}^n)^2+\frac{1}{4}+\frac{\kappa}{2}|\nabla_hU_{j+\frac{1}{2},k+\frac{1}{2}}^n|^2\Big)\Delta x\Delta y\\
&\ge\sum_{j=1}^{N_x}\sum_{k=1}^{N_y}\Big((U_{j,k}^n)^2-\frac{9}{4}+\frac{1}{4}+\frac{\kappa}{2}|\nabla_hU_{j+\frac{1}{2},k+\frac{1}{2}}^n|^2\Big)\Delta x\Delta y\\
&\ge C_0\|U^n\|_{H^1,h}^2-2L_1L_2,
\end{aligned}$$

where $C_0=\min(1,\kappa/2)$. Therefore it holds that

$$\|U^n\|_{H^1,h}^2\le\frac{1}{C_0}\big(E_h(U^0)+2L_1L_2\big).\tag{2.9}$$

By the following discrete Sobolev Lemma [22], there exists a constant $C_1>0$ such that

$$\|f\|_\infty \le C_1\|f\|_{H^1,h}. \tag{2.10}$$

Combining the inequalities (2.9) and (2.10) leads to the result (2.8), which implies the proposed scheme (2.3) is unconditionally stable in L^∞-norm. □

2.3 Error estimate

Assume that

$$C_2=\max_{j,k,n}\{|U^n_{j,k}|,|u^n_{j,k}|\},$$

where $U^n_{j,k}$ is the finite difference solution and $u^n_{j,k}=u(x_j,y_k,t^n)$ is the exact solution of the Cahn-Hilliard equation. It is noted that such C_2 exists because the proposed scheme is unconditionally stable in L^∞-norm. Denote the pointwise error by

$$e^n_{j,k}=U^n_{j,k}-u^n_{j,k}.$$

Lemma 2.3. *The following estimate holds for the nonlinear terms in the scheme* (2.3)

$$\begin{aligned}&\Big\|\frac{(U^{n+1})^2+(U^n)^2}{2}\frac{U^{n+1}+U^n}{2}-\frac{U^{n+1}+U^n}{2}-\big(u^{n+\frac12}\big)^3+u^{n+\frac12}\Big\|_h^2\\ \le&(1+3(C_2)^2)^2\big(\|e^{n+1}\|_h^2+\|e^n\|_h^2\big)+\frac{(C_2)^2}{4}\big\|\eta^{n+\frac12}\big\|_h^2+4(1+3(C_2)^2)^2\big\|\theta^{n+\frac12}\big\|_h^2,\end{aligned} \tag{2.11}$$

where

$$\eta^{n+\frac12}_{j,k}=\big(u^{n+1}_{j,k}-u^n_{j,k}\big)^2,\qquad \theta^{n+\frac12}_{j,k}=u^{n+\frac12}_{j,k}-\frac{u^{n+1}_{j,k}+u^n_{j,k}}{2}.$$

Proof.

$$\frac{(U^{n+1}_{j,k})^2+(U^n_{j,k})^2}{2}\frac{U^{n+1}_{j,k}+U^n_{j,k}}{2}-\frac{U^{n+1}_{j,k}+U^n_{j,k}}{2}-\big(u^{n+\frac12}_{j,k}\big)^3+u^{n+\frac12}_{j,k}=I_1+I_2+I_3+I_4, \tag{2.12}$$

where

$$\begin{aligned}I_1&=\Big(\frac{(U^{n+1}_{j,k})^2+(U^n_{j,k})^2}{2}-1\Big)\frac{U^{n+1}_{j,k}+U^n_{j,k}}{2}-\Big(\frac{(u^{n+1}_{j,k})^2+(U^n_{j,k})^2}{2}-1\Big)\frac{u^{n+1}_{j,k}+U^n_{j,k}}{2},\\ I_2&=\Big(\frac{(u^{n+1}_{j,k})^2+(U^n_{j,k})^2}{2}-1\Big)\frac{u^{n+1}_{j,k}+U^n_{j,k}}{2}-\Big(\frac{(u^{n+1}_{j,k})^2+(u^n_{j,k})^2}{2}-1\Big)\frac{u^{n+1}_{j,k}+u^n_{j,k}}{2},\\ I_3&=\Big(\frac{(u^{n+1}_{j,k})^2+(u^n_{j,k})^2}{2}-1\Big)\frac{u^{n+1}_{j,k}+u^n_{j,k}}{2}-\Big(\Big(\frac{u^{n+1}_{j,k}+u^n_{j,k}}{2}\Big)^2-1\Big)\frac{u^{n+1}_{j,k}+u^n_{j,k}}{2},\\ I_4&=\Big(\Big(\frac{u^{n+1}_{j,k}+u^n_{j,k}}{2}\Big)^2-1\Big)\frac{u^{n+1}_{j,k}+u^n_{j,k}}{2}-\Big(\Big(u^{n+\frac12}_{j,k}\Big)^2-1\Big)u^{n+\frac12}_{j,k}.\end{aligned}$$

$$
\begin{aligned}
I_1 &= \Big(\frac{(U_{j,k}^{n+1})^2+(U_{j,k}^n)^2}{2}-1\Big)\frac{U_{j,k}^{n+1}+U_{j,k}^n}{2}-\Big(\frac{(u_{j,k}^{n+1})^2+(U_{j,k}^n)^2}{2}-1\Big)\frac{u_{j,k}^{n+1}+U_{j,k}^n}{2}\\
&=\frac{(U_{j,k}^{n+1})^2+(U_{j,k}^n)^2}{2}\frac{U_{j,k}^{n+1}+U_{j,k}^n}{2}-\frac{(U_{j,k}^{n+1})^2+(U_{j,k}^n)^2}{2}\frac{u_{j,k}^{n+1}+U_{j,k}^n}{2}\\
&\quad+\frac{(U_{j,k}^{n+1})^2+(U_{j,k}^n)^2}{2}\frac{u_{j,k}^{n+1}+U_{j,k}^n}{2}-\frac{(u_{j,k}^{n+1})^2+(U_{j,k}^n)^2}{2}\frac{u_{j,k}^{n+1}+U_{j,k}^n}{2}-\frac{e_{j,k}^{n+1}}{2}\\
&=\frac{(U_{j,k}^{n+1})^2+(U_{j,k}^n)^2}{2}\frac{e_{j,k}^{n+1}}{2}+\frac{u_{j,k}^{n+1}+U_{j,k}^n}{2}\frac{(U_{j,k}^{n+1})^2-(u_{j,k}^{n+1})^2}{2}-\frac{e_{j,k}^{n+1}}{2}.
\end{aligned}
$$

It follows that

$$|I_1|\le\frac{1}{2}(1+3(C_2)^2)|e_{j,k}^{n+1}|. \tag{2.13}$$

By the similar trick, we can get

$$|I_2|\le\frac{1}{2}(1+3(C_2)^2)|e_{j,k}^{n}| \tag{2.14}$$

and

$$|I_4|\le(1+3(C_2)^2)\Big|u_{j,k}^{n+\frac{1}{2}}-\frac{u_{j,k}^{n+1}+u_{j,k}^n}{2}\Big|, \tag{2.15a}$$

$$
\begin{aligned}
I_3 &= \Big(\frac{(u_{j,k}^{n+1})^2+(u_{j,k}^n)^2}{2}-1\Big)\frac{u_{j,k}^{n+1}+u_{j,k}^n}{2}-\Big(\Big(\frac{u_{j,k}^{n+1}+u_{j,k}^n}{2}\Big)^2-1\Big)\frac{u_{j,k}^{n+1}+u_{j,k}^n}{2}\\
&=\frac{u_{j,k}^{n+1}+u_{j,k}^n}{2}\Big(\frac{(u_{j,k}^{n+1})^2+(u_{j,k}^n)^2}{2}-\Big(\frac{u_{j,k}^{n+1}+u_{j,k}^n}{2}\Big)^2\Big)\\
&=\frac{u_{j,k}^{n+1}+u_{j,k}^n}{2}\frac{(u_{j,k}^{n+1}-u_{j,k}^n)^2}{4}.
\end{aligned} \tag{2.15b}
$$

Then it holds that

$$|I_3|\le\frac{C_2}{4}(u_{j,k}^{n+1}-u_{j,k}^n)^2. \tag{2.16}$$

Combining (2.13)-(2.16), we get

$$\Big\|\frac{(U^{n+1})^2+(U^n)^2}{2}\frac{U^{n+1}+U^n}{2}-\frac{U^{n+1}+U^n}{2}-\big(u^{n+\frac{1}{2}}\big)^3+u^{n+\frac{1}{2}}\Big\|_h^2\le\sum_{i=1}^4 4\|I_i\|_h^2.$$

Then (2.11) holds. □

Theorem 2.4. *If the Cahn-Hilliard system* (1.1a)-(1.1c) *has a solution* $u(\boldsymbol{x},t)\in C^6(\Omega\times[0,T])$, *then the numerical solution of the finite difference system* (2.3) *converges to the exact solution with the rate*

$$\|e^n\|_h=\mathcal{O}\big((\Delta t)^2+(\Delta x)^2+(\Delta y)^2\big).$$

Proof. It is easy to get the error equation as below

$$\frac{e_{j,k}^{n+1}-e_{j,k}^{n}}{\Delta t}=\Delta_h\Big(\Big(\frac{(U_{j,k}^{n+1})^2+(U_{j,k}^{n})^2}{2}-1\Big)\frac{U_{j,k}^{n+1}+U_{j,k}^{n}}{2}-\kappa\Delta_h\frac{e_{j,k}^{n+1}+e_{j,k}^{n}}{2}$$
$$-\big(u_{j,k}^{n+\frac{1}{2}}\big)^3+u_{j,k}^{n+\frac{1}{2}}+\kappa\zeta_{j,k}^{n+\frac{1}{2}}\Big)+\xi_{j,k}^{n+\frac{1}{2}},\tag{2.17}$$

where

$$\zeta_{j,k}^{n+\frac{1}{2}}=\Delta u_{j,k}^{n+\frac{1}{2}}-\Delta_h\frac{u_{j,k}^{n+1}+u_{j,k}^{n}}{2},$$
$$\xi_{j,k}^{n+\frac{1}{2}}=\Big(\frac{\partial u}{\partial t}\Big)_{j,k}^{n+\frac{1}{2}}-\frac{u_{j,k}^{n+1}-u_{j,k}^{n}}{\Delta t}+\Delta\mu_{j,k}^{n+\frac{1}{2}}-(\Delta_h\mu)_{j,k}^{n+\frac{1}{2}}.$$

Let

$$F_{j,k}^{n+\frac{1}{2}}=\Big(\frac{(U_{j,k}^{n+1})^2+(U_{j,k}^{n})^2}{2}-1\Big)\frac{U_{j,k}^{n+1}+U_{j,k}^{n}}{2}-\kappa\Delta_h\frac{e_{j,k}^{n+1}+e_{j,k}^{n}}{2}-\big(u_{j,k}^{n+\frac{1}{2}}\big)^3+u_{j,k}^{n+\frac{1}{2}}+\kappa\zeta_{j,k}^{n+\frac{1}{2}}.$$

Multiplying $\Delta t\frac{e_{j,k}^{n+1}+e_{j,k}^{n}}{2}$ to both sides of (2.17) and summing for $j=1,\cdots N_x$ and $k=1,\cdots N_y$ gives

$$\frac{\|e^{n+1}\|_h^2-\|e^{n}\|_h^2}{2\Delta t}=\Big(\Delta_h F^{n+\frac{1}{2}},\frac{e^{n+1}+e^{n}}{2}\Big)_h+\Big(\xi^{n+\frac{1}{2}},\frac{e^{n+1}+e^{n}}{2}\Big)_h.\tag{2.18}$$

Also we have the estimate for F as

$$\frac{1}{\kappa}\big(F^{n+\frac{1}{2}},F^{n+\frac{1}{2}}\big)_h=\frac{1}{\kappa}\Big(F^{n+\frac{1}{2}},\Big(\frac{(U^{n+1})^2+(U^{n})^2}{2}-1\Big)\frac{U^{n+1}+U^{n}}{2}$$
$$-\big(u^{n+\frac{1}{2}}\big)^3+u^{n+\frac{1}{2}}-\kappa\Delta_h\frac{e^{n+1}+e^{n}}{2}+\kappa\zeta^{n+\frac{1}{2}}\Big)_h.\tag{2.19}$$

Adding Eqs. (2.18), (2.19) and noting that by periodic boundary condition

$$\Big(\Delta_h F^{n+\frac{1}{2}},\frac{e^{n+1}+e^{n}}{2}\Big)_h=\Big(F^{n+\frac{1}{2}},\Delta_h\frac{e^{n+1}+e^{n}}{2}\Big)_h,\tag{2.20}$$

we get

$$\begin{aligned}&\frac{\|e^{n+1}\|_h^2-\|e^{n}\|_h^2}{2\Delta t}+\frac{1}{\kappa}\|F^{n+\frac{1}{2}}\|_h^2\\&=\frac{1}{\kappa}\Big(F^{n+\frac{1}{2}},\Big(\frac{(U^{n+1})^2+(U^{n})^2}{2}-1\Big)\frac{U^{n+1}+U^{n}}{2}-\big(u^{n+\frac{1}{2}}\big)^3+u^{n+\frac{1}{2}}+\kappa\zeta^{n+\frac{1}{2}}\Big)_h\\&\quad+\Big(\xi^{n+\frac{1}{2}},\frac{e^{n+1}+e^{n}}{2}\Big)_h\\&\le\frac{1}{\kappa}\|F^{n+\frac{1}{2}}\|_h^2+\frac{1}{4\kappa}\Big\|\Big(\frac{(U^{n+1})^2+(U^{n})^2}{2}-1\Big)\frac{U^{n+1}+U^{n}}{2}-\big(u^{n+\frac{1}{2}}\big)^3+u^{n+\frac{1}{2}}+\kappa\zeta^{n+\frac{1}{2}}\Big\|_h^2\\&\quad+\Big(\xi^{n+\frac{1}{2}},\frac{e^{n+1}+e^{n}}{2}\Big)_h.\end{aligned}\tag{2.21}$$

It follows that

$$\begin{aligned}
&\frac{\|e^{n+1}\|_h^2-\|e^n\|_h^2}{\Delta t}\\
\leq&\frac{1}{2\kappa}\Big\|\Big(\frac{(U^{n+1})^2+(U^n)^2}{2}-1\Big)\frac{U^{n+1}+U^n}{2}-\big(u^{n+\frac{1}{2}}\big)^3+u^{n+\frac{1}{2}}+\kappa\zeta^{n+\frac{1}{2}}\Big\|_h^2\\
&+\big(\xi^{n+\frac{1}{2}},e^{n+1}+e^n\big)_h\\
\leq&\frac{\|e^{n+1}\|_h^2+\|e^n\|_h^2}{2}+\frac{1}{\kappa}\Big\|\Big(\frac{(U^{n+1})^2+(U^n)^2}{2}-1\Big)\frac{U^{n+1}+U^n}{2}-\big(u^{n+\frac{1}{2}}\big)^3+u^{n+\frac{1}{2}}\Big\|_h^2\\
&+\kappa\|\zeta^{n+\frac{1}{2}}\|_h^2+\|\xi^{n+\frac{1}{2}}\|_h^2\\
\leq&\Big(\frac{1}{2}+\frac{(1+3(C_2)^2)^2}{\kappa}\Big)\big(\|e^{n+1}\|_h^2+\|e^n\|_h^2\big)+\frac{(C_2)^2}{4\kappa}\|\eta^{n+\frac{1}{2}}\|_h^2+\frac{4(1+3(C_2)^2)^2}{\kappa}\|\theta^{n+\frac{1}{2}}\|_h^2\\
&+\kappa\|\zeta^{n+\frac{1}{2}}\|_h^2+\|\xi^{n+\frac{1}{2}}\|_h^2.
\end{aligned}\tag{2.22}$$

Summing both sides with respect to n, we get

$$\begin{aligned}
\|e^n\|_h^2\leq\|e^0\|_h^2+\sum_{k=0}^{n}\Delta t\Big(1+\frac{2(1+3(C_2)^2)^2}{\kappa}\Big)\|e^k\|_h^2+\sum_{k=0}^{n-1}\Delta t\Big(\frac{(C_2)^2}{4\kappa}\|\eta^{k+\frac{1}{2}}\|_h^2\\
+\frac{4(1+3(C_2)^2)^2}{\kappa}\|\theta^{k+\frac{1}{2}}\|_h^2+\kappa\|\zeta^{k+\frac{1}{2}}\|_h^2+\|\xi^{k+\frac{1}{2}}\|_h^2\Big).
\end{aligned}\tag{2.23}$$

Let

$$\Delta t\Big(1+\frac{2(1+3(C_2)^2)^2}{\kappa}\Big)\leq\frac{1}{2}$$

or equivalently,

$$\Delta t\leq\Big[2+\frac{4(1+3(C_2)^2)^2}{\kappa}\Big]^{-1}.\tag{2.24}$$

By Taylor expansion, it is easy to get the following four estimations:

$$\begin{aligned}
\zeta_{j,k}^{n+\frac{1}{2}}=&\frac{(\Delta x)^2}{12}\frac{\partial^4u}{\partial x^4}(x_1,y_k,t^{n+\frac{1}{2}})+\frac{(\Delta y)^2}{12}\frac{\partial^4u}{\partial x^4}(x_j,y_1,t^{n+\frac{1}{2}})+\frac{(\Delta t)^2}{8}\Big(\frac{\partial^4u}{\partial x^2\partial t^2}(x_2,y_k,t_2)\\
&+\frac{\partial^4u}{\partial y^2\partial t^2}(x_j,y_2,t_2)\Big),\quad t_n<t_2<t_{n+1},\ x_{j-1}<x_1,x_2<x_{j+1},\ y_{k-1}<y_1,y_2<y_{k+1},
\end{aligned}\tag{2.25a}$$

$$\begin{aligned}
\xi_{j,k}^{n+\frac{1}{2}}=&\frac{(\Delta t)^2}{24}\frac{\partial^3u}{\partial t^3}(\boldsymbol{x}_{j,k},t_1)-\frac{(\Delta x)^2}{12}\frac{\partial^4\mu}{\partial x^4}(x_3,y_k,t^{n+\frac{1}{2}})-\frac{(\Delta y)^2}{12}\frac{\partial^4\mu}{\partial y^4}(x_j,y_3,t^{n+\frac{1}{2}}),\\
&t_n<t_1<t_{n+1},\ x_{j-1}<x_3<x_{j+1},\ y_{k-1}<y_3<y_{k+1},
\end{aligned}\tag{2.25b}$$

$$\theta_{j,k}^{n+\frac{1}{2}}=\frac{(\Delta t)^2}{8}\frac{\partial^2u}{\partial t^2}(\boldsymbol{x}_{j,k},t_3),\qquad t_n<t_4<t_{n+1},\tag{2.25c}$$

$$\eta_{j,k}^{n+\frac{1}{2}}=(\Delta t)^2\Big(\frac{\partial u}{\partial t}(\boldsymbol{x}_{j,k},t_4)\Big)^2,\quad t_n<t_4<t_{n+1}.\tag{2.25d}$$

From (2.25a)-(2.25d), there exists a constant C_3 such that

$$\begin{aligned}&\frac{(C_2)^2}{4\kappa}\|\eta^{k+\frac{1}{2}}\|_h^2+\frac{4(1+3(C_2)^2)^2}{\kappa}\|\theta^{k+\frac{1}{2}}\|_h^2+\kappa\|\zeta^{k+\frac{1}{2}}\|_h^2+\|\xi^{k+\frac{1}{2}}\|_h^2\\ \leq&C_3|\Omega|((\Delta x)^2+(\Delta y)^2+(\Delta t)^2)^2.\end{aligned}\tag{2.26}$$

From (2.23) and (2.26) and under the condition (2.24), by Gronwall's inequality [22], we get the following error estimate

$$\|e^n\|_h\leq\sqrt{\|e^0\|_h^2+C_3|\Omega|T}e^{\left(1+\frac{2(1+3(C_2)^2)^2}{\kappa}\right)T}\left((\Delta x)^2+(\Delta y)^2+(\Delta t)^2\right).\tag{2.27}$$

Thus, the theorem is proved. □

3 Adaptive time-stepping method

In the previous sections, we have proved that the nonlinear scheme (2.3) is unconditionally energy stable and L^∞-norm stable which implies large time steps are allowed. However, for the sake of accuracy, very large time step is unacceptable except in the time intervals where the solution variation is very small. Our numerical experiments also show that long time simulations using large constant time steps may produce nonphysical solutions at intermediate time stages (i.e., wrong dynamics), although the large time physical behaviors are less sensitive to the time steps used. As we know, at the early stage of dynamics of the Cahn-Hilliard model, the corresponding energy decays quickly because of the nonlinear interaction, and then the energy decays rather slowly until it reaches a steady state. Based on these observations, we are motivated to use adaptive time steps. It is reasonable to adjust the time step in the following form,

$$\Delta t=\max\left(\Delta t_{\min},\frac{\Delta t_{\max}}{\sqrt{1+\alpha|E'(t)|^2}}\right),\quad \alpha \text{ is a constant,}\tag{3.1}$$

where E is the energy functional defined in the model. The constant α is chosen in experience and it is used to adjust the level of adaptivity.

The introduction of the pre-set smallest time step $\Delta t_{\min}$ is to force the adaptive time steps bounded from below by $\Delta t_{\min}$ to avoid too small time steps. Likewise, $\Delta t_{\max}$ gives the upper bound of the time steps. Consequently,

$$\Delta t_{\min}\leq\Delta t\leq\Delta t_{\max}.$$

Moreover, large $|E'(t)|$ will lead to the small time step, which corresponds to the case of rapid decay of energy or quick motion of the structural transition from one stage to the immediate next one. Similarly, small $|E'(t)|$ yields the large time step, which corresponds to the slow motion of the phase interface. $\Delta t_{\min}$ is relevant to the time intervals of the most rapid energy decay, and $\Delta t_{\max}$ corresponds to the time intervals of the slowest

energy decay. In our computation, we choose $\Delta t_{\min} = a\kappa$ with $0.1 \le a \le 1$ and $\Delta t_{\max} = b\kappa$ with $1 \le b \le 100$. In theory, $\Delta t_{\max}$ may be infinity, but for practical computation, we give it a reasonable bound. The large time steps can be used in the computation since the energy stability and the mass conservation are preserved of the proposed finite difference scheme in this paper. This time-stepping strategy has been successfully utilized in the long time numerical simulations of the epitaxial growth models in [15] with different finite difference schemes.

4 Numerical experiments

We use the Newton iteration method to solve the discrete nonlinear system (2.3). The tolerance for the iteration is set to be 10^{-8}. The numerical solution at the previous time level is taken as the initial guess at each time step. The algebraic multigrid method is used to solve the linearized system at each Newton iterative step. The tolerance for the multigrid method is also set to be 10^{-8}.

Example 4.1. The initial condition is taken as the trigonometric function with very small amplitude,

$$u_0(x,y) = 0.05 \sin x \sin y,$$

and the problem is subject to periodic boundary condition. The parameter κ in (1.1a)-(1.1c) is 0.01. $\Omega = [0,2\pi] \times [0,2\pi]$.

This example is designed to study the accuracy and the efficiency of the adaptive stepping method. First, we test the numerical accuracy in time. Since the exact solution is unknown, we take the numerical result obtained on a 400×400 mesh and the time step $\Delta t = 0.0001$ as the "exact" solution. Table 1 shows the L^2-errors obtained using different constant time steps. It is seen that for this two-dimensional Cahn-Hilliard problem the numerical scheme (2.3) gives $\mathcal{O}(\Delta t^2)$ error in L^2-norm.

Table 1: Example 4.1: L^2-errors with different constant time steps.

Δt	0.01	0.005	0.0025	0.00125
$\|e\|$	1.3384E-6	3.3461E-7	8.6344E-8	2.2297E-9

In Fig. 1, we plot the solution contour lines for some selected time levels. The space grid is taken as 200×200 and the adaptive time step follows the indicator defined in (3.1) with $\Delta t_{\min} = 0.001$, $\Delta t_{\max} = 0.1$ and $\alpha = 100$. It is observed from these figures that the solution has a quick motion in the early stage of the evolution, and it develops slowly later until it reaches a steady state. It can also be reflected from the energy evolution which is presented in Fig. 2.

In Fig. 2, we present the numerical energies obtained using different parameter settings in (3.1). The parameter α in (3.1) is very important for choosing appropriate time

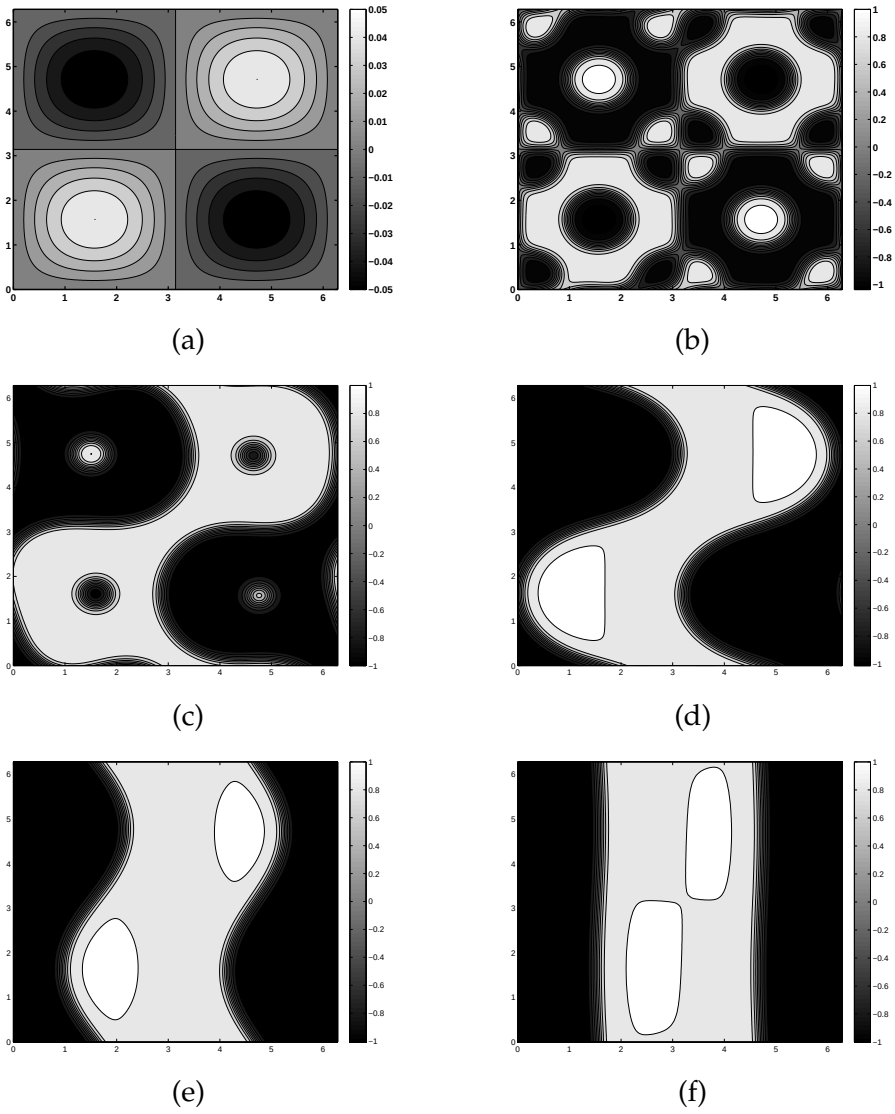

Figure 1: Example 4.1: Numerical solutions obtained using scheme (2.3) at (a) $t=0$; (b) $t=2$; (c) $t=6$; (d) $t=10$; (e) $t=50$; (f) $t=100$.

steps. For this problem, $100\leq\alpha\leq500$ is a good choice, although we tried a large range of this parameter. Here, we only provide the results with $\alpha=100$ and $\alpha=500$. Too large α will lead to too small time steps (almost equal to $\Delta t_{\min}$), and then there will be no improvement of computation efficiency. Too small α will produce rather large time steps, consequently it will bring poor accuracy. Both energy curves in the left of Fig. 2 for $1\leq t\leq7$ will almost coincide for longer time, so only one of them (corresponding to $\alpha=500$) is plotted in the right of Fig. 2 to show the long time development of the energy.

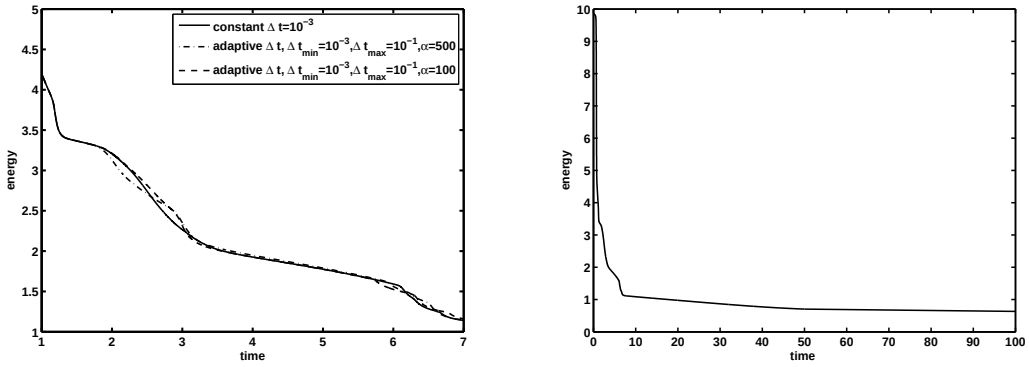

Figure 2: Example 4.2: energy evolution for $1\leq t\leq 7$ (left) and $0\leq t\leq 100$ (right).

In order to further study the efficiency of the adaptive time-stepping strategy, we list the CPU time (in seconds) consumed using different parameters in (3.1) and using constant time steps, respectively. It is seen from Table 2 that the computation time is greatly saved when using adaptive time step selection, especially after $t=10$. This is due to the slow decay of the energy after $t=10$.

Table 2: Example 4.1: CPU time (seconds) comparison. The adaptive time step is determined by (3.1) with $\Delta t_1=(\Delta t_{\max}=0.1,\Delta t_{\min}=0.001,\alpha=100)$ and $\Delta t_2=(\Delta t_{\max}=0.1,\Delta t_{\min}=0.001,\alpha=500)$. The constant time step $\Delta t=0.001$.

t	2	4	10	30	70	100	300	600
adaptive Δt_1	4001	8473	17761	24623	40763	42361	52013	129720
adaptive Δt_2	4059	8559	18058	26261	42492	51472	60925	171509
constant Δt	4092	9005	19668	51378	116435	160768	449757	889739

In Fig. 3, we plot the adaptive time steps against time. Corresponding to the early stage of the development, we have small time steps, which are produced by the relatively

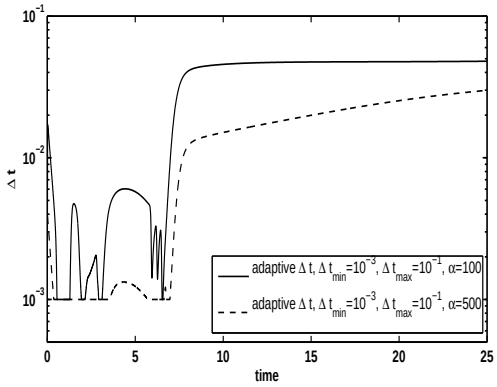

Figure 3: Example 4.1: time step evolution for $0\leq t\leq 25$ with different parameters.

sharp decay of the energy. Then after $t=10$ the time steps become larger and larger because the energy decreases slowly, and by the time step indicator (3.1), larger time steps are determined.

Example 4.2. The initial condition is a random state by assigning a random number varying from -0.05 to 0.05 to each grid point. We take the parameter κ as $\kappa=0.001$, and the domain is $\Omega=[0,2\pi]\times[0,2\pi]$.

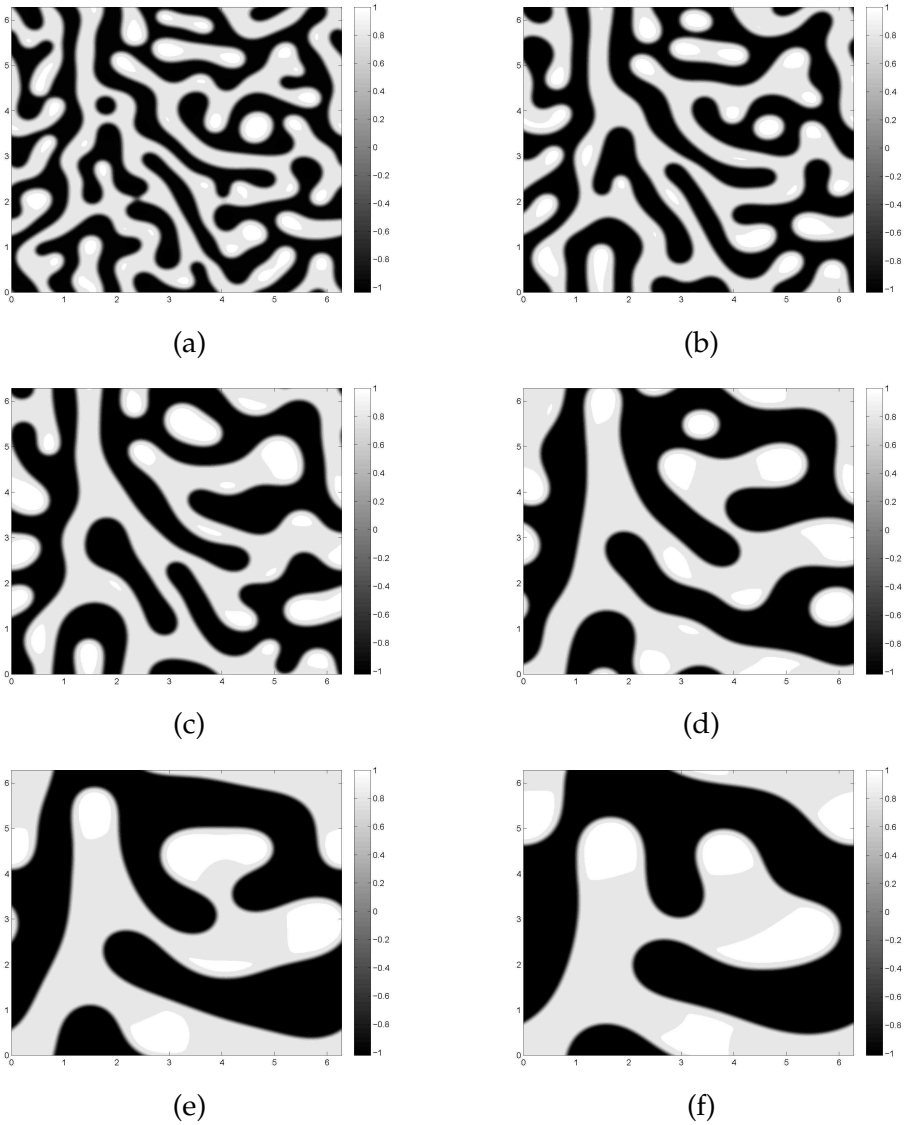

Figure 4: Example 4.2: Numerical solutions obtained using scheme (2.3) and adaptive time steps (3.1) with $\Delta t_{\max}=0.1$, $\Delta t_{\min}=0.0001$, $\alpha=50$. (a) $t=0.5$; (b) $t=1$; (c) $t=2$; (d) $t=5$; (e) $t=10$; (f) $t=20$.

The physical domain is partitioned with a 200×200 uniform grid. The adaptive time step indicator defined in (3.1) is applied here with $\Delta t_{\max}=0.1$, $\Delta t_{\min}=0.0001$, $\alpha=50$. Actually, we have tried different values for the parameter α. There is no distinguish difference of the solutions when $50\leq\alpha\leq200$, so we only present the numerical results with $\alpha=50$. In Fig. 4, we plotted the contour lines in some selected time levels.

The energy curves are presented in Fig. 5 obtained using adaptive time steps and constant time steps, respectively. It is observed that the two curves almost coincides except minor difference. Therefore, our strategy for choosing adaptive time step does not lose much accuracy numerically. In Fig. 6, we plot the time step distribution throughout the development of the solution for $0\leq t\leq20$. During the initial stage of the evolution of the solution, small time steps are determined and later larger time steps are produced. This is due to the essential property of the energy of the Cahn-Hilliard equation: the energy decays quickly in the early time and decays slowly later.

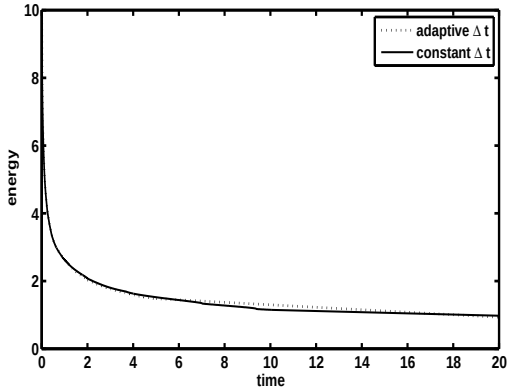

Figure 5: Example 4.2: Energy development for $0\leq t\leq20$. The adaptive time step (3.1) is used with $\Delta t_{\max}=0.1$, $\Delta t_{\min}=0.0001$, $\alpha=50$. The constant time step is taken as $\Delta t=0.0001$.

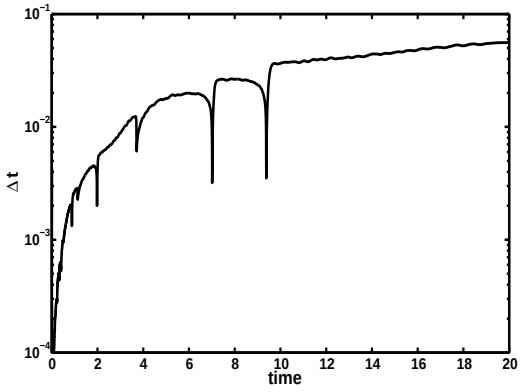

Figure 6: Example 4.2: adaptive time step evolution.

5 Conclusions

In this work, we have developed and analyzed an unconditionally energy stable finite difference scheme for solving the two-dimensional Cahn-Hilliard equation. The error estimate for the numerical solution is also obtained with the order $\mathcal{O}\big((\Delta x)^2+(\Delta y)^2+(\Delta t)^2\big)$.

Since the scheme is unconditionally energy stable, large time steps are allowed in the long time numerical simulations. However, constant large time steps may cause accuracy loss. So we proposed an adaptive time-stepping strategy. The energy is used to monitor the change of the time steps. Large time steps are used when the energy decays rapidly and small time steps are adopted otherwise. For the adaptive time-stepping strategy, variable time steps may be employed from time to time. For this regard, multilevel schemes may not be useful. The finite difference scheme proposed in this paper is a one-step method, which is found appropriate for the time adaptivity. Numerical experiments demonstrated that the adaptive time stepping approach can greatly save CPU time without losing accuracy.

Acknowledgments

We would like to thank Prof. Houde Han of Tsinghua University and Prof. Qiang Du of Penn State University for their helpful discussions. Z. R. Zhang was supported by National NSF of China under Grant 10601007. Z. H. Qiao was supported by the FRG grants of the Hong Kong Baptist University under Grant No. FRG2/09-10/034.

References

[1] J. W. Cahn and J. E. Hilliard, Free energy of a non-uniform system I: interfacial free energy, J. Chem. Phys., 28 (1958), 258–267.
[2] J. Carr, M. E. Curtin and M. Slemrod, Structured phase transitions on a finite interval, Arch. Rat. Mech. Anal., 86 (1984), 317–351.
[3] M. W. Cheng and J. A. Warren, Controlling the accuracy of unconditionally stable algorithms in the Cahn-Hilliard equation, Phys. Rev. E, 75 (2007), 017702.
[4] S. M. Choo, S. K. Chung and K. I. Kim, Conservative nonlinear difference scheme for the Cahn-Hilliard equation-II, Comput. Math. Appl., 39 (2000), 229–243.
[5] Q. Du and R. A. Nicolaides, Numerical analysis of a continuum model of phase transition, SIAM J. Numer. Anal., 28 (1994), 1310–1322.
[6] C. M. Elliott and Z. Sonqmu, On the Cahn-Hilliard equation, Arch. Rat. Meth. Anal., 96 (1986), 339–357.
[7] C. M. Elliott and D. A. French, Numerical studies of the Cahn-Hilliard equation for phase separation, IMA J. Appl. Math., 38 (1987), 97–128.
[8] C. M. Elliott and D. A. French, A nonconforming finite element method for the two-dimensional Cahn-Hilliard equations, SIAM J. Numer. Anal., 26 (1989), 884–903.

[9] C. M. Elliott and S. Larsson, Error estimates with smooth and nonsmooth data for a finite element method for the Cahn-Hilliard equation, Math. Comput., 58 (1992), 603–630.
[10] D. Furihata, A stable and conservative finite difference scheme for the Cahn-Hilliard equation, Numer. Math., 87 (2001), 675–699.
[11] Y. N. He, Y. X. Liu and T. Tang, On large time-stepping methods for the Cahn-Hilliard equation, Appl. Numer. Math., 57 (2007), 616–628.
[12] C. Liu and J. Shen, A phase field model for the mixture of two incompressible fluids and its approximation by a Fourier-spectral method, Phys. D, 179 (2003), 211–228.
[13] S. E. Minkoff and N. M. Kridler, A comparison of adaptive time stepping methods for coupled flow and deformation modeling, Appl. Math. Model., 30 (2006), 993–1009.
[14] A. Novick-Cohen and L. A. Segel, Nonlinear aspects of the Cahn-Hilliard equation, Phys. D, 10 (1984), 277–298.
[15] Z. H. Qiao, Z. R. Zhang and T. Tang, An adaptive time-stepping strategy for the epitaxial growth models, SIAM J. Sci. Comput., 33 (2011), 1395–1414.
[16] G. Söderlind, Automatic control and adptive time-stepping, Numer. Algor., 31 (2001), 281–310.
[17] Z. Z. Sun, A second-order accurate linearized difference scheme for the two-dimensional Cahn-Hilliard equation, Math. Comput., 64 (1995), 1463–1471.
[18] Z. J. Tan, Z. R. Zhang, T. Tang and Y. Q. Huang, Moving mesh methods with locally varying time steps, J. Comput. Phys., 200 (2004), 347–367.
[19] S. M. Wise, Unconditionally stable finite difference, nonlinear multigrid simulation of the Cahn-Hilliard-Hele-Shaw system of equations, J. Sci. Comput., 44 (2010), 38–68.
[20] C. J. Xu and T. Tang, Stability analysis of large time-stepping methods for epitaxial growth models, SIAM J. Numer. Anal., 44 (2006), 1759–1779.
[21] S. Zhang and M. Wang, A nonconforming finite element method for Cahn-Hilliard equation, J. Comput. Phys., 229 (2010), 7361–7372.
[22] Y. L. Zhou, Applications of Discrete Functional Analysis to the Finite Difference Method, International Academic Publishers, 1990.